On the variation of b-values with earthquake size

Emile A. Okal [a,*], Barbara A. Romanowicz [b]

[a] *Department of Geological Sciences, Northwestern University, Evanston, IL 60208, USA*
[b] *Seismographic Station, University of California, Berkeley, CA 94720, USA*

Abstract

We investigate the effect on Gutenberg and Richter's parameter b of the saturation of moment–magnitude relationships caused by source finiteness. Any conventional magnitude scale measured at a constant period features a saturation which results in a stepwise increase in the slope of the $\log_{10}$ moment–magnitude relationship. We predict that this leads to an increase in b value with earthquake size. This is in addition to the effect of the physical saturation of the transverse dimension of the fault, previously described in the literature. A number of scaling models are used to predict the behavior of b with increasing magnitude, in the case of both the 20 s surface-wave magnitude M_s, and the 1 s body-wave magnitude m_b. We show in particular that a b value of unity can be expected only in a range of earthquake size where the relevant magnitude has already started to saturate: it should be the exception, not the rule, and cannot be extended to a wide range of magnitudes, except at the cost of significant curvature in the frequency–magnitude curve. The widely reported $b = 1$ stems from the common practice of using a heterogeneous magnitude scale, e.g. M_s for large events and m_b for smaller ones.

1. Introduction and background

The purpose of this paper is to explore theoretically, and test on a number of datasets, the variation of the frequency–magnitude coefficient b with earthquake size, owing to the influence of source finiteness effects on magnitude–moment relationships. We will describe populations of shallow earthquakes (with depths $h \leq 75$ km) and model them according to Gutenberg and Richter's (1954) relationship

$$\log_{10} N = a - bM \tag{1}$$

where M is a particular magnitude scale, and N is the number of events in the group whose magnitude is greater than M. Because of the logarithmic nature of (1), a similar relationship is found, with the same value of b, when using the number of shocks dn in the magnitude window $\{M, M + dM\}$. Throughout this paper, a will denote a constant whose actual value may vary from equation to equation.

The longstanding interest in b values goes back to Gutenberg and Richter (1941), who first noticed the 'rule of tenfold increase', and soon after defined b through Eq. (1), proposing $b = 0.9$ for shallow shocks and various values greater than unity for deeper events (Gutenberg and Richter, 1954). In a more modern framework, the

* Corresponding author.

b value of a population of earthquakes has been related to the fractal dimension D of the source, under the hypothesis that the process of faulting is scale-invariant. Turcotte (1992) has proposed $D = 1.8$ on the basis of $b = 0.9$ for shallow earthquakes, based on Gutenberg and Richter's (1954) figure.

We refer to a recent study by Frohlich and Davis (1993) for a review and perspective on previous work regarding b values. These workers discussed the influence of a number of parameters on teleseismic b values. However, in all cases, they constrained themselves to a 'limited' range of earthquake sizes, rarely exceeding one unit of magnitude. This underscores the difficulty in obtaining stable results (in other words, a good linear fit between $\log_{10} N$ and M) over broad ranges of earthquake sizes.

This situation can be described and analyzed in the formalism of Rundle (1989), who proposed the following three-step argument to justify a b value of unity:

(1) In a population of earthquakes, it is assumed that the process of faulting is scale independent. Then the number of shocks of a given size, dn, is inversely proportional to their rupture area, S.

(2) Scaling laws predict a dependence of the form $S = M_0^\beta$ between area and seismic moment M_0, leading to

$$\log_{10} N = a - \beta \log_{10} M_0 \qquad (2)$$

(3) The magnitude M involved in the frequency–magnitude relationship scales as

$$M = a + \alpha \log_{10} M_0 \qquad (3)$$

Under those conditions, one predicts a b value

$$b = \frac{\beta}{\alpha} \qquad (4)$$

For relatively moderate earthquakes involving no saturation of their dimensions, scaling laws predict $\beta = 2/3$ (e.g. Geller, 1976); in addition, a slope of two-thirds is often assumed between M and the logarithm (base ten) of the seismic moment, and hence $b = 1$.

In a series of recent papers (Pacheco et al., 1992; Romanowicz and Rundle, 1993), it has been pointed out that a significant change in b value

results from the inability of fault dimensions, notably fault width W, to keep growing indefinitely with increasing earthquake size. As a result, a significant increase in b value is observed around $\log_{10} M_0 = 27.2$ (Pacheco et al., 1992), which Romanowicz and Rundle (1993) have interpreted as expressing the simultaneous saturation of W and of the slip Δu on the fault. In this so-called 'W model' (Scholz, 1982), the length of faulting L is the only parameter which keeps increasing with earthquake size (in the alternate 'L model', the slip would keep increasing with L after W has saturated). Both $M_0 = \mu \cdot L W_S \cdot \Delta u_S$ and $S = L \cdot W_S$ (where the subscript S indicates a saturating variable) then grow proportionally to L, leading to $\beta = 1$ instead of $2/3$.

An additional and significant limitation to the derivation of $b = 1$ from Eqs. (1)–(4) is the fact that $\alpha = 2/3$ applies only in a very specific range of earthquake sizes for any given magnitude scale M measured at a fixed period $T = 2\pi/\omega_T$. For example, when considering the 20 s magnitude M_s, it applies only in the range $6.76 \le M_s \le 8.12$, when the reference angular frequency $\omega_{20} = 2\pi/20$ rad s^{-1} is already past the corner frequency relative to the length L of the source, but remains smaller than those involving the rise time τ and the width W of the fault (Geller, 1976). As many 'interesting' (i.e. large but not gigantic) earthquakes occur in this regime, Kanamori (1977) chose to involve a factor of two-thirds when introducing his energy magnitude M_w, which was designed to recast the computed value of a seismic moment in terms of the more familiar concept of magnitude:

$$M_w = \tfrac{2}{3} \log_{10} M_0 - 10.73 \qquad (5)$$

In other words, the domain where $\alpha = 2/3$ is also that where M_w coincides with M_s. For smaller earthquakes involving no saturation of M_s, it has long been observed that magnitudes M_w computed from (5) significantly overestimate M_s (see, e.g. Ekström and Dziewonski, 1986), and a linear relationship ($\alpha = 1$) between M_s and $\log_{10} M_0$ is both predicted theoretically (Okal, 1989) and observed (Ekström and Dziewonski, 1986; Okal, 1989). Under those circumstances, (4) predicts that b should drop from 1 to $2/3$.

In the present paper, we explore theoretically the predicted variations of b with earthquake size owing to the influence of source finiteness on magnitude, both in the case of M_s and of the 1 s body-wave magnitude m_b, and compare them with observed b values computed from several datasets including the Harvard centroid moment tensor (CMT) catalog, and the National Earthquake Information Center (NEIC) database. In doing so, we hope to shed some additional light on the confused question of b values and their variation with magnitude(s). To our knowledge, the influence on b values of the variation of α with earthquake size has not been discussed (or adequately separated from that of β) in the literature.

2. Frequency–moment relationships: β values

As explained above, there are two fundamentally different reasons why b values should vary with earthquake size. The variation in β expresses a genuine physical change in the nature and scaling of the earthquake source; the variation in α merely expresses the inherent incapacity of conventional magnitudes to describe large earthquakes properly. In this respect, β values (referred to as b' values by Romanowicz (1992); see also Molnar (1979)) are of course physically more meaningful than b values, and could conceivably become more universal, given that seismic moments, now published routinely, have become the preferred descriptor of earthquake size.

Table 1
β Values predicted and observed in this study

Dataset or model	No. of samples	Moment range ($\log_{10}$) (dyn cm)	β value	Reference (Fig.)
Predicted theoretically				
W model		< 27.2	2/3	
		> 27.2	1	
L model		< 27.2	2/3	
		> 27.2	1/2	
Observed (this study)				
CMT catalog 1977–1992	8015	> 24.2	0.79	
		24.2–27.2	0.70	Fig. 1
		> 27.2	1.31	Fig. 1
First half	4008	24.2–27.2	0.69	Fig. 2(a)
		> 27.2	1.08	Fig. 2(a)
Second half	4007	24.2–27.2	0.71	Fig. 2(b)
		> 27.2	1.42	Fig. 2(b)
Odd only	4008	24.2–27.2	0.69	Fig. 2(c)
		> 27.2	1.04	Fig. 2(c)
Even only	4007	24.2–27.2	0.70	Fig. 2(d)
		> 27.2	1.54	Fig. 2(d)
Thrust	3694	24.2–27.2	0.64	Fig. 3(a)
		> 27.2	1.53	Fig. 3(a)
Normal	1201	24.2–28.0	0.73	Fig. 3(b)
Strike-slip	1822	24.4–25.7	0.71	Fig. 3(c)
		25.8–27.1	0.79	Fig. 3(c)
		> 27.1	1.15	Fig. 3(c)
Odd	1298	24.2–26.5	0.69	Fig. 3(d)
		26.5–28	0.85	Fig. 3(d)
PPT (M_m) catalog 1987–1991	391	25.2–27.2	0.59	Fig. 6(b)
		> 27.2	1.18	Fig. 6(b)
CMT catalog 1977–1992 ($m_b \geq 4.5$)	8011	> 24.2	0.79	
'No-M_s', events in CMT catalog	1583	> 24	0.83	
		24.2–27.2	0.70	
		> 27.2	1.32	

We refer to Romanowicz and Rundle (1993) for a derivation of the theoretical values

$$\beta = \tfrac{2}{3} \quad (M_0 < M_0^c) \tag{6a}$$

$$\beta = 1 \quad (M_0 > M_0^c) \tag{6b}$$

In particular, these authors have shown that the so-called 'L model' (in which the slip Δu is controlled by the fault length L and hence does not saturate with fault width (Scholz, 1982)) would lead to a decrease ($\beta = 1/2$) rather than an increase of β at large moment ranges. As for the critical moment, M_0^c in (6), it can be related to the saturated fault width W_S, by using an appropriate scaling law, e.g. Geller's (1976) model of a buried fault:

$$M_0^c = 2\mu\epsilon_{max} \cdot W_S^3 = \Delta\sigma W_S^3 \tag{7}$$

where ϵ_{max} is the rupture strain of the material, or equivalently, $\Delta\sigma$ is the earthquake's stress drop. If $\Delta\sigma = 50$ bars, the observed value ($\log_{10} M_0^c = 27.2$) suggests $W_S = 30$ km. In the case of a fault breaking the surface, the two in (7) would be replaced by a factor four. Width saturation at the same physical depth would double the value of M_0^c. Conversely, it is probably illusory to envision a saturation depth W_S defined world-wide with a precision better than 25% (a multiplicative factor $2^{1/3}$), and thus we will simply assume a buried fault in the following discussion.
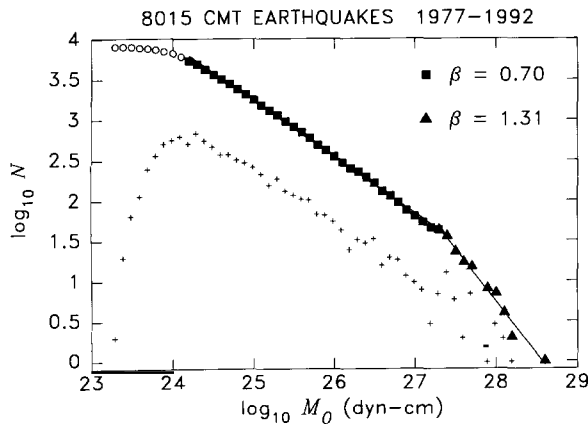

Fig. 1. Frequency–moment relationship for the dataset of shallow ($h \le 75$ km) events from the CMT catalog. (See text for details).

2.1. Comparison with data

Following in the footsteps of Pacheco et al. (1992) and Romanowicz and Rundle (1993), we study the frequency–moment relationship for the Harvard CMT catalog. Our database, shown in Fig. 1, consists of all 8015 events with shallow centroid depth ($h \le 75$ km), for the years 1977–1992, with results summarized in Table 1.

In this and all subsequent figures, the width of the sorting bins is 0.1 unit of $\log_{10} M_0$ (or of magnitude). Individual crosses represent the number of earthquakes in each bin; the other symbols relate to the cumulative number N, i.e. to the number of events with moments M_0 or greater (or with magnitudes M or greater). β values (or b values) are obtained by fitting a straight line to $\log_{10} N$ over specific ranges of moment (or magnitude). Different symbols are used for different ranges, and the corresponding value of β (or b) printed on the right. Open circles denote parts of the dataset not used in the regressions, principally at low moment (or magnitude) ranges, where the completeness of the dataset would be questionable. In all cases, the figures are log–log plots with common scales, so that $-\beta$ (or $-b$) is also the true slope of the regression on the figure.

The change of β value previously described by Pacheco et al. (1992) is of course immediately apparent in Fig. 1, with the lower moment population ($\beta = 0.70$) following closely its predicted behavior ($\beta = 2/3$). We address the issue of the robustness of the results through several experiments. First, we consider only the first and second halves of the dataset, split at their mid-point in time, 9 April, 1986. Second, we split the dataset into its even and odd numbers, and study those populations separately (Fig. 2). The following conclusions can be drawn from our results:

(1) Our study is in agreement with the W model, as β is found to undergo a sharp increase at the critical moment M_0^c.

(2) For $M_0 < M_0^c$, the slope $\beta = 2/3$ predicted by the theory is also confirmed to within a few hundredths of a unit. This slope is practically constant over three orders of magnitude of M_0

suggesting that the physical nature of the scaling of the source does not change below M_0^c.

(3) The value of the critical moment, $M_0^c = (1.5-2) \times 10^{27}$ dyn-cm, suggests a saturation width $W_c = 30-33$ km, which would correspond to a penetration depth $h = 21-23$ km, under the assumption of a dip $\delta = 45°$ of the fault plane.

(4) For $M_0 > M_0^c$, and owing to the relatively small size of the population, the value of β is much less robust. In particular, it is to a large extent controlled by the largest event in the dataset, the 1977 Indonesian earthquake: any data subset including this event yields β values in generally good agreement with the expected value of 1.0; sub-datasets excluding the event result in higher β values, of the order of 1.4. However, we do observe that β increases beyond M_0^c to values of the order of, or larger than, unity, which is in agreement with the W model.

(5) We also wish to comment briefly on an older study by Chinnery and North (1975), who obtained a β value of 0.61 (in excellent agree-

ment with the figure of 2/3 expected theoretically), over the full range of moments extending beyond 10^{30} dyn-cm. In other words, these researchers did not find evidence for a critical moment, and a change of β value at large moments. This discrepancy with modern results is due to their practice of using as 'moments' (e.g. in their Fig. 3) estimates based on interpreting reported magnitudes (either M_s or older scales such as M_{PAS}): this procedure is notoriously unreliable for large events, due to the scatter in the M_s–M_0 relationship above 10^{28} dyn-cm.

The fact that the β value is exactly two-thirds in the domain of earthquake sizes where the faulting is scale-invariant indicates that the fractal dimension D of shallow earthquakes is exactly two.

2.2. Influence of focal mechanism

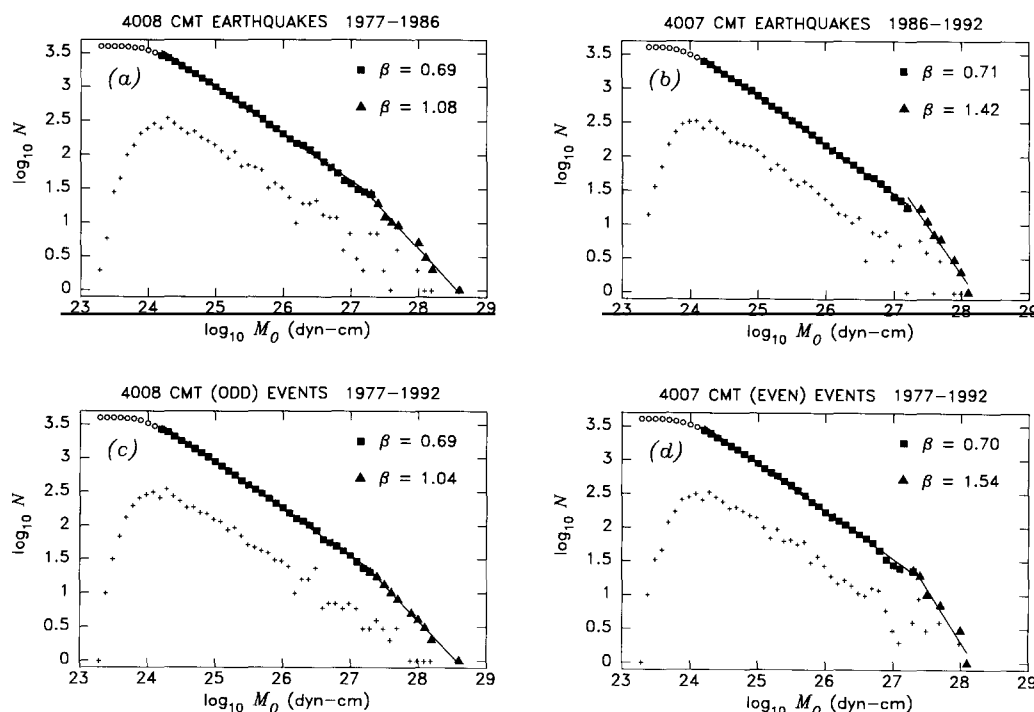In this section, we investigate the extent to which the above results could be affected by the

Fig. 2. Robustness tests run on the Fig. 1 dataset. (a) and (b), first and second halves of the dataset; (c) and (d), odd and even parts of the dataset. (Note that the results are very robust for the lower moment range, less so for the larger moment range.)

nature of faulting (strike-slip, thrust, normal, etc.). We are motivated both by the obvious fact that the saturation of W may take place under different physical constraints for different geometries, and by the work of Frohlich and Davis (1993), who have reported variations in b values between earthquakes with differing focal mechanisms. However, for each of the populations they considered, their analyses were restricted to relatively narrow ranges of earthquake size, which would not allow a systematic study of the variation of b values with magnitude. It should be noted also that these workers used b values computed on the moment magnitude M_w: physically, these represent β values, and should be interpreted as such after multiplication by two-thirds. Following Frohlich and Apperson (1992), we sorted the 8015 events in the dataset into strike-slip, normal, thrust, and 'odd' mechanisms, depending on which, if any, of the moment tensor's principal axes is close to the vertical. To allow a direct comparison with Frohlich and Davis' (1993) re-

sults, we use their less stringent definition of thrust faults (T axis within $\delta_T = 40°$ of the vertical, as opposed to 30° for the other families; however, our results would not be altered by taking $\delta_T = 30°$). Results are given in Table 1 and Fig. 3.

(1) The behavior of the thrust family of sources is basically the same as that of the whole CMT dataset. This is not surprising given the mere number of such events (3694 out of 8015, or 46%), which clearly control the whole population. Our results are also in agreement with Frohlich and Davis' (1993), derived for a narrow window below M_0^c: their b value of 0.86 for M_w would correspond to $\beta = 0.57$.

(2) Normal faulting earthquakes exhibit a different behavior. Fig. 3(b) shows no clear-cut evidence of a change in β values. It must be emphasized that only three (out of a total of 1201) events have a moment larger than the critical moment for the whole population ($M_0^c = 1.5 \times 10^{27}$ dyn cm), and thus the question of the behav-
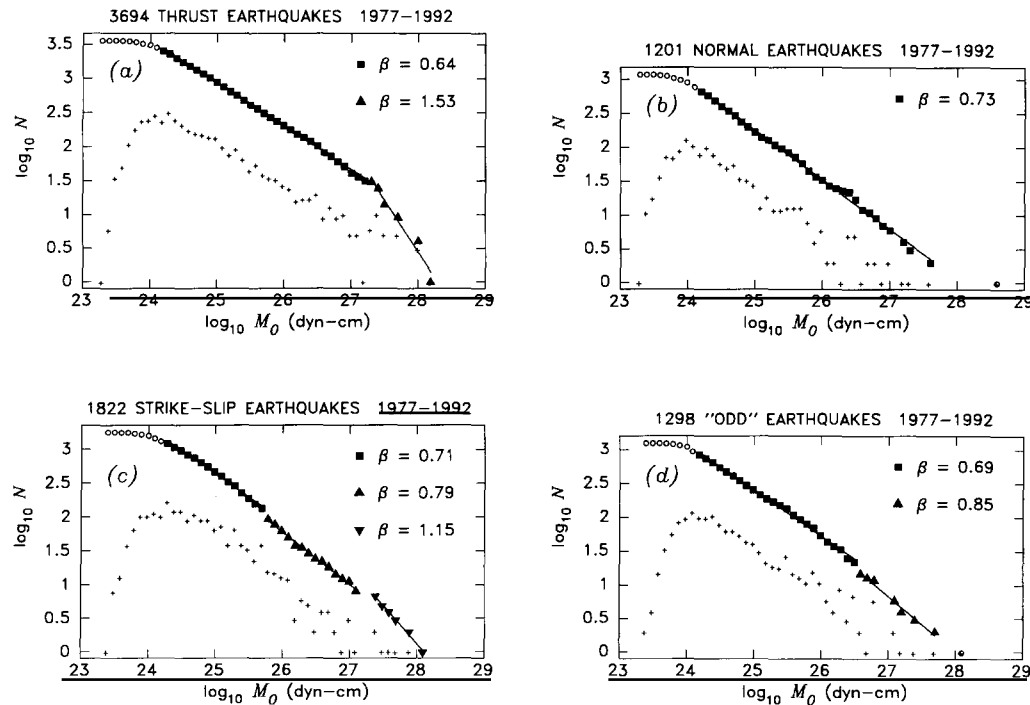

Fig. 3. Frequency–moment relationship for the CMT dataset, sorted by focal mechanism, according to the classification of Frohlich and Apperson (1992).

ior of β beyond M_0^c remains indeterminate. At any rate, and with the exception of the largest event, the population is very well fitted by a straight line with a slope $\beta = 0.73$, only slightly greater than the value two-thirds predicted in the absence of width saturation. The largest earthquake is of course the Indonesian event of 19 August 1977; it has been described either as a decoupling event involving seismic rupture of the entire lithospheric plate (Given and Kanamori, 1980) or as a source with anomalously high stress drop but restricted fault dimensions (Fitch et al., 1981; Silver and Jordan, 1983). In both cases (albeit for different reasons), it would not be expected to fit the W model of Romanowicz and Rundle (1993): a high stress drop would violate any scaling model relating W to M_0; a rupture of the entire lithospheric plate would obviously violate the concept of a shallow limit to the transverse extent W of the fault. Extending either of these properties to the whole population of normal faulting earthquakes would explain the constancy of β values throughout the moment range. Our results are in excellent agreement with Frohlich and Davis' (1993) $b = 1.06$ ($\beta = 0.71$).

(3) The case of the 1822 strike-slip events is more intriguing. As shown in Fig. 3(c), a significant increase in β value with seismic moment is documented, but a sharp elbow is not easily defined: although at lower ranges of M_0, β approaches two-thirds, the transition to higher values is smooth. This observation would suggest that the critical fault width W_S is not unique among strike-slip earthquakes, as would be expected from the variety of tectonic environments in which they occur.

(a) Along transform segments of the mid-ocean ridge system, the saturating depth, controlled by temperature, will be a function of both spreading rate and transform offset, but in all cases will remain very small, at most 10 km. Indeed, the frequency–moment relationship for the 828 such events exhibits considerable curvature and cannot be properly fitted by a straight line, even for smaller earthquakes (Fig. 4(a)).

(b) We similarly process in Fig. 4(b) the 630 strike-slip events occurring in subduction environments. These earthquakes generally correspond
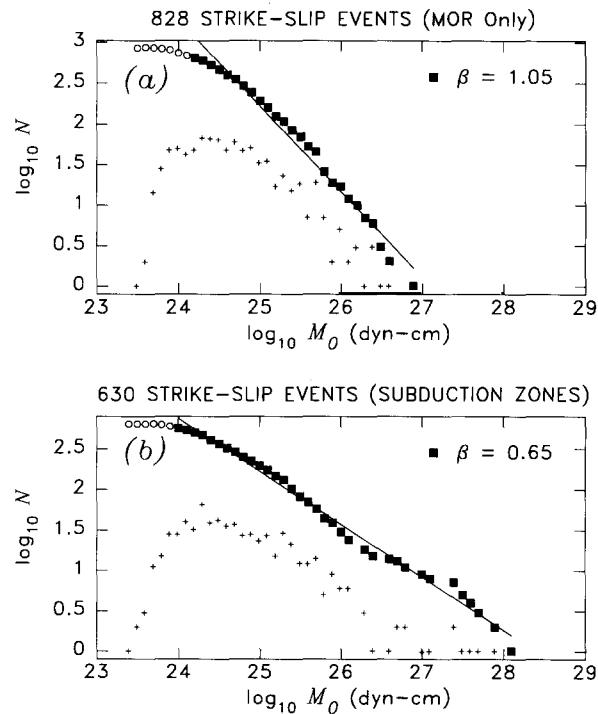

Fig. 4. Frequency–moment relationship for the sub-dataset of strike-slip CMT solutions with epicenters on the mid-ocean ridge system (a) and in subduction environments (b). (Note that neither can be fitted well by a single straight line.)

to complex tectonic regimes, such as plate kinematic conditions varying rapidly over short distances (as in the case of the Macquarie region), decoupled strike-slip motion in convergent zones (as in the case of Western New Guinea), etc.; many are found to occur at significant depth (beyond 50 km). The frequency–moment relationship is a complex one, with a lack of earthquakes in the range 10^{26}–10^{27} dyn cm. It cannot be fitted well by a straight line.

(c) That leaves a dataset of 364 strike-slip events which occurred mostly on well-defined major continental strike-slip faults (Fig. 5(a)), including such systems as the San Andreas fault, the Sumatra fault, the Motagua fault, and the Anatolian and other major Asian strike-slip faults. These faults are expected to be well modeled by a ribbon-like structure, whose width is controlled by the thermal regime of the continental lithosphere, but whose length is limited only by the

364 STR.–SLIP EVENTS (MOR and SUBD. Zones Excepted)
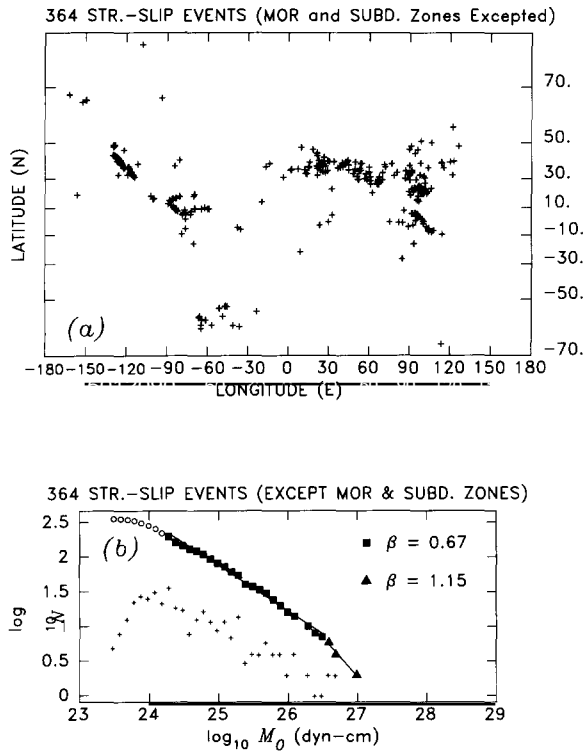

364 STR.–SLIP EVENTS (EXCEPT MOR & SUBD. ZONES)

Fig. 5. (a) Distribution of strike-slip events belonging neither to the mid-ocean ridge system nor to subduction environments. (b) Frequency–moment relationship for the dataset plotted in (a). (Note slope of two-thirds at low moments, and critical moment significantly smaller than for the global dataset on Fig. 1.)

lateral extent of the tectonic province. As shown in Fig. 5(b), the frequency–moment relationship for this group is very well fitted by the theoretical

value $\beta = 2/3$ in the range $\log_{10} M_0 \leq 26.5$; beyond this, there is some suggestion of an increase in β value, but the number of events involved (six) is very small; the corresponding value of the corner moment would translate into a maximum depth of 17.5 km, under the assumption of a vertical fault, and of a stress drop $\Delta\sigma = 50$ bars. This figure is in agreement with the depth of maximum seismicity along the San Andreas fault system.

Our β values for strike-slip events are generally larger than found by Frohlich and Davis (1993). This discrepancy may reflect the fact that we cover a much broader range of moments, with the strike-slip dataset exhibiting significant curvature.

(4) Finally, the frequency–moment pattern for the 1298 earthquakes with 'odd' mechanisms is unclear: no evidence for a sharp change of regime is seen, but a single fit by a straight line ($\beta = 0.76$) leaves significant curvature (Fig. 3(d)). The dataset is fitted reasonably well ($\beta = 0.69$) for $\log_{10} M_0 \leq 26.5$. At higher moments, the slope increases only modestly. Significantly, the largest two events in this family have been described as involving unusual features: Lundgren and Okal (1988) have proposed that the 1977 Tonga earthquake ($M_0 = 1.4 \times 10^{28}$ dyn cm) involved a substantial vertical rupture, and Lundgren et al. (1989) have argued that the 1986 Kermadec event ($M_0 = 4.5 \times 10^{27}$ dyn cm) had an anomalously high stress release, both situations violating the assumptions used in the derivation of the behav-

Table 2

b Values predicted and observed in this study (mantle magnitude M_m)

Dataset or model	No. of samples	Magnitude range	b value	Reference (Fig.)
Predicted theoretically				
W model		< 7.2	2/3	
		> 7.2	1	
L model		< 7.2	2/3	
		> 7.2	1/2	
Observed (this study)				
PPT (M_m) catalog 1987–1991	391	5.2–7.2	0.62	Fig. 6(a)
		> 7.2	0.97	Fig. 6(a)
PPT (M_c) catalog 1987–1991	391	5.2–7.2	0.60	Fig. 6(c)
		> 7.2	1.28	Fig. 6(c)

ior of β. Our lower-moment β value remains in good agreement with Frohlich and Davis' (1993) $b = 1.05$ ($\beta = 0.70$).

3. Application to magnitude scales; b values

3.1. The mantle magnitude M_m

In any range of earthquake sizes for which a given magnitude scale is unaffected by source finiteness, $\alpha = 1$, and hence, $b = \beta$. In particular, this should be the case over all magnitude ranges, for the mantle magnitude M_m, introduced by Okal and Talandier (1989). In this respect, it appeared interesting to study the catalog of mantle magnitudes M_m routinely obtained at Papeete (PPT) since 1987, and described most recently by Hyvernaud et al. (1993). This catalog contains 391 events with $h \le 75$ km. We conducted three experiments on this dataset, the results of which are presented in Table 2 and Fig. 6.

First, we investigated the b value resulting from the use of the mantle magnitude M_m. It is clear from Fig. 6(a) that although routine processing of events is attempted above $M_m = 4$, the dataset is probably complete only for $M_m \ge 5.2$. That this figure is significantly higher than for the Harvard CMT dataset is due at least in part to the single-station nature of the PPT dataset, resulting in a geographic bias for smaller events: at lower moments, only those events sufficiently close to PPT will be processed, whereas at larger moments the dataset acquires a world-wide character; on the other hand, with a world-wide network, there are always at least a few stations close to the epicenter, and no bias exists. With this in mind, we used a lower threshold of 5.2 in the b value regression. The resulting b value diagram clearly shows a change of behavior at $M_m = 7.2$, with slopes of 0.62 and 0.98, respectively. These values are very close to the theoretical ones, two-thirds and unity.

Second, we investigated directly the β values of the dataset by regressing the Harvard CMT moments published for the earthquakes in the PPT catalog. The result at low moments, $\beta = 0.59$, is in good agreement with the b value, whereas
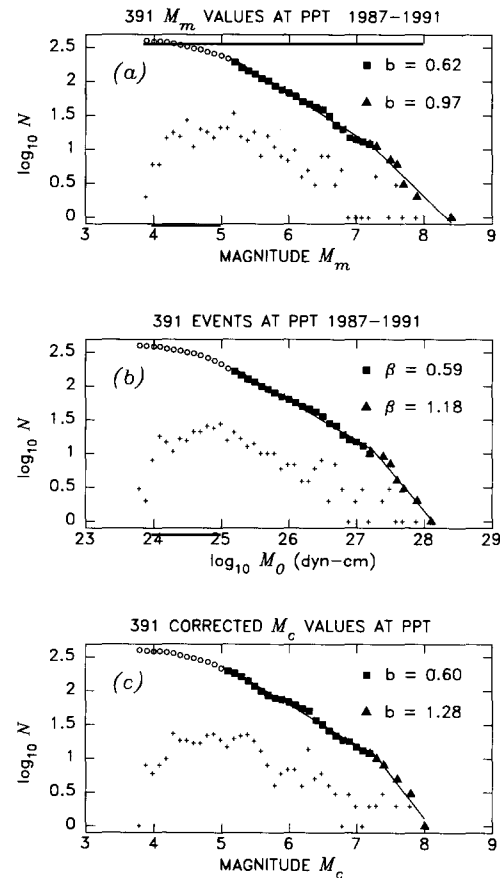

Fig. 6. Frequency–size relationship for the dataset of 391 shallow events used by Hyvernaud et al. (1992). (a) b-values resulting from the use of the mantle magnitude M_m; (b) corresponding β values obtained for the same dataset by using the moment values reported in the CMT catalog; (c) b values resulting from the use of the corrected magnitude M_c (see text for details).

the deviation of b from β for large events illustrates the very small number of earthquakes considered. In general, the good agreement between b and β is an expression of the fact that the residuals ($r = M_m - \log_{10} M_0 + 20$) do not exhibit any systematic variation with earthquake size (Okal and Talandier, 1989; Hyvernaud et al., 1993).

Finally, we investigated the possible effect of neglecting the event's focal geometry in the M_m algorithm on the resulting b value. For this purpose, we analyzed the 'corrected' M_c values, as

defined by Okal and Talandier (1989), and listed for the PPT dataset in Hyvernaud et al. (1993). As would be expected, the results are in generally excellent agreement with the β values; the only significant difference with M_m is the larger b value beyond fault width saturation, which results from a substantial correction in the case of the 1989 Macquarie Ridge earthquake, whose M_m value was overestimated at PPT, owing to focal geometry. At any rate, as this involves a single event, it is not statistically significant.

3.2. The 20 s surface-wave magnitude M_s

The relationship between M_s and M_0 has long been known to involve an additional pattern of saturation, which results in a variation of the constant α in Eq. (3) with earthquake size (e.g.

Geller, 1976). This takes place in several steps, which can be modeled by the following relations:

$$M_s = \log_{10} M_0 - 19.46 \quad (M_s < 6.7) \tag{8a}$$

$$M_s = \tfrac{2}{3} \log_{10} M_0 - 10.73 \quad (6.7 \le M_s \le 8.0) \tag{8b}$$

$$M_s = \tfrac{1}{3} \log_{10} M_0 - 1.36 \quad (8.0 \le M_s \le 8.22) \tag{8c}$$

$$M_s = 8.22 \quad (M_0 \ge 10^{28} \text{ dyn-cm}) \tag{8d}$$

obtained by combining the models of Geller (1976), Ekström and Dziewonski (1986) and Okal (1989). It should be emphasized, however, that Geller's theory assumes uniform scaling for earthquake faults of all sizes, and does not accommodate a physical saturation of source parameters, either in a W or an L model. In the Appendix, we discuss this issue and give a tentative justification of (8). At any rate, Fig. 7 shows that these relationships give a satisfactory fit both
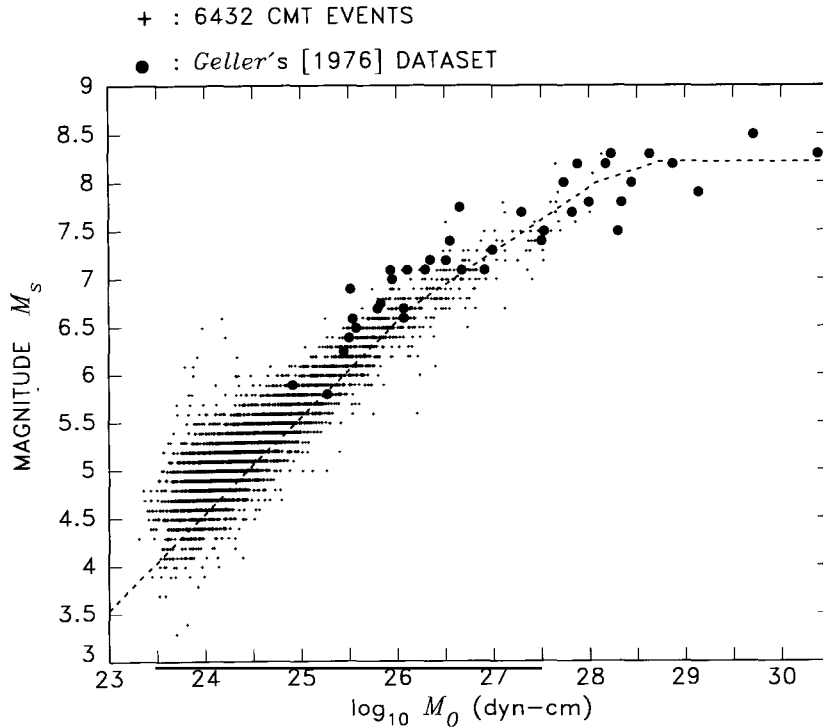

Fig. 7. Magnitude M_s vs. published moment, for shallow CMT events (+), and for Geller's (1976) dataset of 41 large shallow earthquakes (●). The dashed line represents the relationship between M_s and M_0 as modeled by (8).

to the modern CMT dataset used in Section 2, and to Geller's (1976) group of 41 large shallow earthquakes.

Combining (6) and (8), one then predicts the following variation of b values with earthquake size:

$$b = \tfrac{2}{3} \quad \left(M_s \le 6.7;\ \beta = \tfrac{2}{3},\ \alpha = 1\right) \quad (9a)$$

$$b = 1 \quad \left(6.7 \le M_s \le 7.4;\ \beta = \tfrac{2}{3},\ \alpha = \tfrac{2}{3}\right) \quad (9b)$$

$$b = \tfrac{3}{2} \quad \left(7.4 \le M_s \le 8.0;\ \beta = 1,\ \alpha = \tfrac{2}{3}\right) \quad (9c)$$

$$b = 3 \quad \left(8.0 \le M_s \le 8.22;\ \beta = 1,\ \alpha = \tfrac{1}{3}\right) \quad (9d)$$

In principle, values of M_s greater than 8.22 should not be observed, as by then, the 20 s surface-wave magnitude is expected to have fully saturated. Note the very narrow range of the $b = 3$ regime, owing to the near-identity of the two corner frequencies for rise time and width (Geller, 1976; Eqs. (21) and (24). In practice, that regime may rarely be observed.

The above theory can be used to build an expected population of M_s-values. At this point, it is important to note that the frequency–magnitude relationship for this expected population must be fitted by at least three line segments; in other words, it exhibits significant curvature. However, if one regresses this population by a single straight line, say between magnitudes 5.0 and 8.2, the resulting b value, 0.94, is indeed very close to unity (Fig. 8(a)); the fit itself is rather poor, owing to curvature. On the other hand, the use of an L model would predict b values of 2/3, 1, 3/4 and 3/2 in the same M_s-ranges; as a result, the frequency–M_s-relationship would lose its curvature, and would be expected to be fitted rather well by a single straight line, but with a slope $b = 0.76$ (Fig. 8(b)).

Comparison with data

We first targeted for study events belonging to the CMT dataset, to insure that we were working with a population of earthquakes comparable with that analyzed in Section 2. For this purpose, we isolated all 6432 shallow CMT solutions for which an $M_s \ge 3$ is reported in the CMT file, and regressed them for their b value. Results are shown in Fig. 9(a) and 9(b) and Table 3. In addition, we

further analyzed a more extensive dataset of 13 301 M_s values, namely the entire NEIC catalog for shallow earthquakes ($h \le 75$ km) for the years 1968–1991 (before 1968, magnitudes M_s were not assigned systematically), with results presented in Figs. 9(c) and 9(d) and Table 3. Robustness tests similar to those described in Section 2 were also conducted; their results are listed in Table 3.

It should be noted that, as expected in the theoretical framework of the W model, a single-line regression of either dataset yields a b value very close to unity, but at the cost of significant misfit owing to the curvature of the frequency–M_s relationship; once again, this property upholds the W model. When the dataset is fitted by several linear segments, the b values of the first
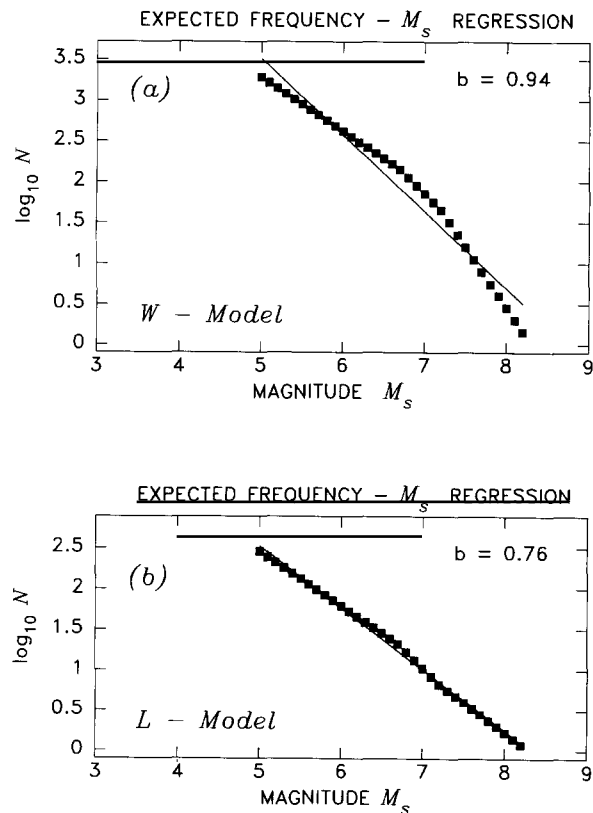

Fig. 8. Frequency–magnitude distributions expected from the combined effects of fault width saturation and of M_s saturation. (a) The W model predicts a b value close to unity, but with significant curvature. (b) The L model predicts a linear relationship, but with a lower b value.

two regimes predicted by (9) are usually very well fitted. A slight difference is found for the b value at higher magnitudes. In the case of the CMT events, a nearly constant regime with $b = 1.86$ is found for $M_s \geq 7.5$; in the case of the larger NEIC dataset, further curvature can be resolved in the frequency–M_s relationship. Finally, the comparison between Figs. 1 and 9(b) which use the same set of earthquakes, illustrates the difference between the physical saturation of the fault width (β values; Fig. 1) and the saturation of the magnitude scale (b values; Fig. 9(b)): the frequency–size distribution in Fig. 9(b) shows more curvature than that in Fig. 1.

3.3. The 1 s body-wave magnitude m_b

In the case of m_b, the situation is changed by the fundamentally different nature of the corner frequency relative to width: as derived by Geller (1976), and because most teleseismic body waves leave at nearly vertical incidence, body waves are

relatively less sensitive to fault width than surface waves, and thus, the width corner frequency is increased by a factor approaching two and differs significantly from the rise time corner frequency. As a result, the domain with $\alpha = 1/3$ extends over a greater range than for surface waves, at the expense of that with $\alpha = 2/3$.

The theoretical relationship between m_b and M_0 for a point-source double-couple has been investigated recently by Okal (1993), who proposed the formula

$$m_b = \log_{10} M_0 - 18.52 \tag{10}$$

based on the analysis of a very large number of synthetic seismograms obtained by ray theory. Because CMT solutions are routinely computed only for events with $m_b \geq 5.0$, a range where m_b is already affected by source finiteness effects, it was not possible to check the performance of (10) against a large dataset in its domain of applicability. It should be noted also that the locking constant in (10) is somewhat different from that
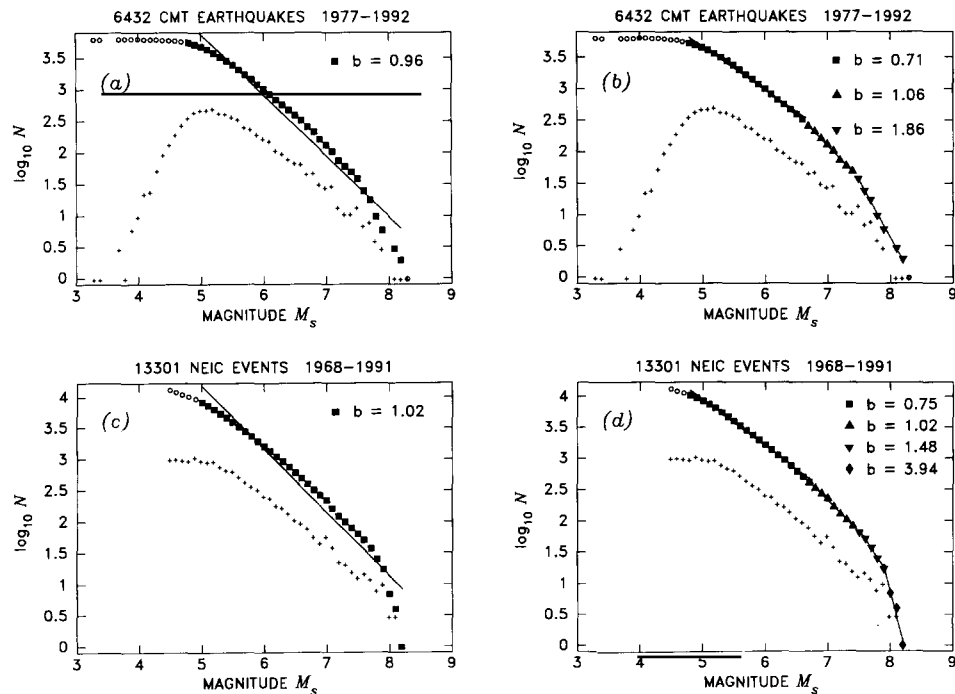

Fig. 9. Top: b value analysis of the shallow CMT dataset using the 20 s surface-wave magnitude M_s: (a) A single segment regression upholds the W model as predicted in Fig. 8(a); (b) segmented regression, as predicted by Eq. (9). Bottom: (c) and (d), same as (a) and (b) for the larger NEIC dataset.

Table 3
b Values predicted and observed in this study (surface-wave magnitude M_s)

Dataset or model	No. of samples	Magnitude range	b value	Reference (Fig.)
Predicted theoretically				
W model		< 6.7	2/3	
		6.7 – 7.4	1	
		7.4 – 8.12	3/2	
		8.12– 8.22	3	
Single regression			0.94	Fig. 8(a)
L model		< 6.7	2/3	
		6.7 – 7.4	1	
		7.4 – 8.12	3/4	
		8.12– 8.22	3/2	
Single regression			0.76	Fig. 8(b)
Observed (this study)				
CMT catalog 1977–1992 ($M_s > 3$)	6432	4.8 – 8.2	0.96	Fig. 9(a)
		4.8 – 6.7	0.71	Fig. 9(b)
		6.7 – 7.4	1.06	Fig. 9(b)
		7.4 – 8.2	1.86	Fig. 9(b)
First half	3216	4.8 – 8.2	0.92	
		4.8 – 6.7	0.70	
		6.7 – 7.4	1.09	
		7.4 – 8.2	2.11	
Second half	3216	4.8 – 8.2	0.92	
		4.8 – 6.7	0.74	
		6.7 – 7.4	1.02	
		7.4 – 8.2	1.26	
Odd only	3216	4.8 – 8.2	0.92	
		4.8 – 6.7	0.71	
		6.7 – 7.4	1.18	
		7.4 – 8.2	1.33	
Even only	3216	4.8 – 8.2	0.92	
		4.8 – 6.7	0.73	
		6.7 – 7.4	0.94	
		7.4 – 8.2	2.42	
NEIC catalog 1968–1991 ($M_s \geq 4.5$)	13301	5.0 – 8.2	1.02	Fig. 9(c)
		4.8 – 6.7	0.75	Fig. 9(d)
		6.7 – 7.4	1.02	Fig. 9(d)
		7.4 – 7.9	1.48	Fig. 9(d)
		7.9 – 8.2	3.94	Fig. 9(d)
First half	6650	4.8 – 8.2	0.92	
		4.8 – 6.7	0.71	
		6.7 – 7.4	1.01	
		7.4 – 7.9	1.33	
		7.9 – 8.2	5.73	
Second half	6651	4.8 – 8.2	0.99	
		4.8 – 6.7	0.81	
		6.7 – 7.4	1.02	
		7.4 – 7.9	1.64	
		7.9 – 8.2	1.73	
Odd only	6651	4.8 – 8.2	0.96	
		4.8 – 6.7	0.75	
		6.7 – 7.4	0.99	
		7.4 – 7.9	1.38	
		7.9 – 8.2	3.13	

Table 3 (continued)

Dataset or model	No. of samples	Magnitude range	b value	Reference (Fig.)
Even only	6650	4.8 – 8.2	0.97	
		4.8 – 6.7	0.75	
		6.7 – 7.4	1.07	
		7.4 – 7.9	1.74	
		7.9 – 8.2	3.89	

given by Geller (1976) at low magnitudes; as a result, we propose to model the dependence of m_b through the following combination of Geller's (1976) and Okal's (1993) results:

$$m_b = \log_{10} M_0 - 18.52 \qquad (m_b \le 4.96) \qquad (11a)$$

$$m_b = \tfrac{2}{3} \log_{10} M_0 - 10.69 \qquad (4.96 \le m_b \le 5.70) \qquad (11b)$$

$$m_b = \tfrac{1}{3} \log_{10} M_0 - 2.50 \qquad (5.70 \le m_b \le 6.40) \qquad (11c)$$

$$m_b = 6.40 \qquad (\log_{10} M_0 \ge 26.7) \qquad (11d)$$

Note that the effect of the physical saturation of W on a possible early saturation of magnitude (as discussed in the Appendix for M_s) does not apply

to m_b, which is expected to have already fully saturated by the time M_0 reaches $M_0^c = 2 \times 10^{27}$ dyn cm.

The CMT database holds 8011 shallow earthquakes ($h \le 75$ km) for which a value of m_b is reported. Fig. 10 shows that (11) provides a reasonable description of the dataset, with the exception of the full saturation at $m_b = 6.4$. This could be due either to measurements taken at periods significantly longer than 1 s, or to earthquakes exhibiting higher than normal stress drops. Accordingly, we will assume that (11c) continues to hold for $\log_{10} M_0 > 26.7$. A single-line regression of the entire dataset yields

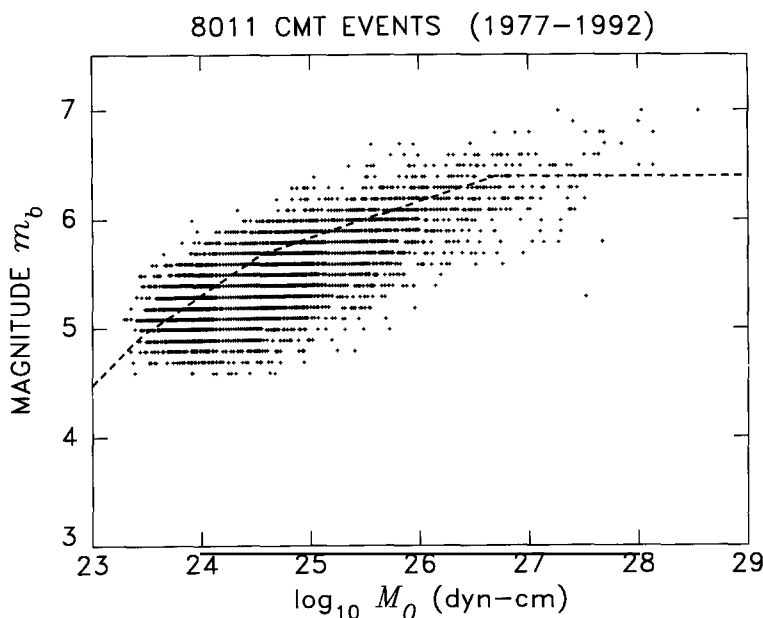$$m_b = 0.37 \log_{10} M_0 - 3.73 \qquad (12)$$

Fig. 10. Body-wave magnitude m_b as a function of moment for the CMT dataset. +, Individual values of m_b taken from the CMT dataset. The dashed line is the theoretical relationship predicted by (11).

with a slope close to one-third. This confirms the predominance of the domain for which $\alpha = 1/3$. The combination of (6) and (11a)–(11c) predicts the following behavior of the frequency–m_b relationship:

$$b = \tfrac{2}{3} \quad \left(m_b \le 5.0; \ \beta = \tfrac{2}{3}; \ \alpha = 1 \right) \tag{13a}$$

$$b = 1 \quad \left(5.0 \le m_b \le 5.7; \ \beta = \tfrac{2}{3}; \ \alpha = \tfrac{2}{3} \right) \tag{13b}$$

$$b = 2 \quad \left(5.7 \le m_b \le 6.6; \ \beta = \tfrac{2}{3}; \ \alpha = \tfrac{1}{3} \right) \tag{13c}$$

$$b = 3 \quad \left(m_b \ge 6.6; \ \beta = 1; \ \alpha = \tfrac{1}{3} \right) \tag{13d}$$

As shown in Fig. 11, the frequency–m_b relationship is expected to show significant curvature, and, if a single straight-line regression is attempted, should yield b values of the order of 1.7–2.0, depending on whether a sufficient population of small events provides adequate coverage of the $b = 2/3$ domain (see Table 4 for details). On the other hand, the L model would predict that b should revert to 1.5 at the larger magnitudes, with straight-line regressions in the range

$b = 1.5$–1.7, and less curvature in the frequency–magnitude diagram.

Comparison with data

We first processed the CMT dataset of 8011 events described above. Fig. 12(a) shows that the dataset is probably complete only for $m_b \ge 5.3$. A single regression carried out above that threshold yields $b = 1.97$, in good agreement with the value predicted by the W model. Regressing the dataset in several steps, as suggested by (13), yields good agreement in the predicted $b = 2$ and $b = 3$ ranges, and a value slightly too large (1.17) for the $b = 1$ range. Tests listed in Table 4 show that the first two b values (1.17 and 1.88) are very robust, whereas the last one is not, varying from two to five depending on which sub-datasets are considered, once again a probable expression of the small populations involved.

We then proceeded to process the entire NEIC dataset (1968–1991) comprising 90 074 events with
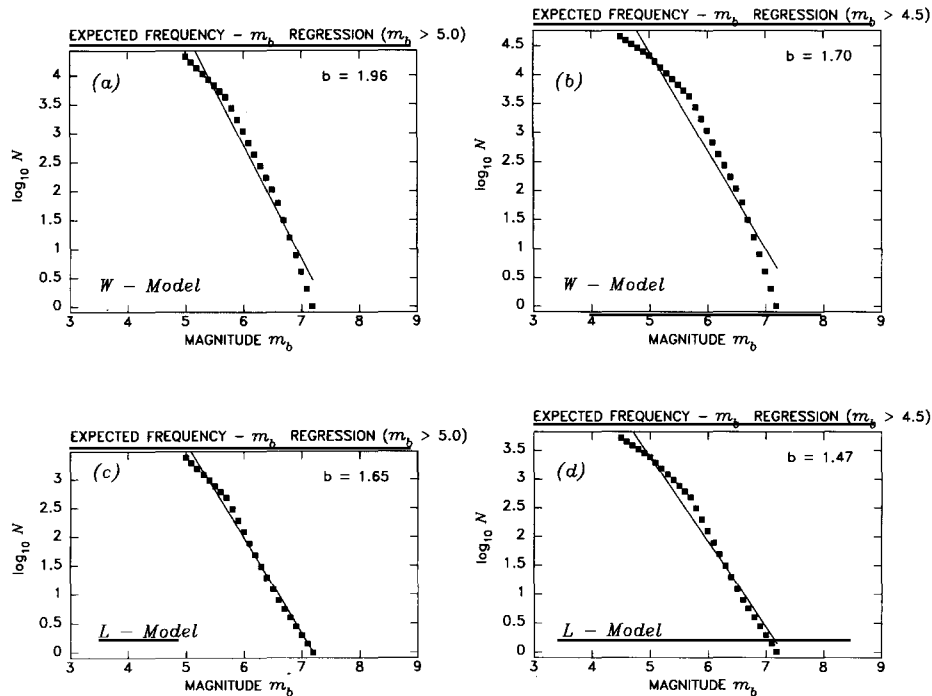

Fig. 11. Same as Fig. 8, for the 1 s body-wave magnitude m_b. The lower bound of m_b is taken as either 5.0 ((a) and (c)) or 4.5 ((b) and (d)) to reflect the different thresholds of the CMT and NEIC catalogs.

Table 4
b Values predicted and observed in this study (body-wave magnitude m_b)

Dataset or model	No. of samples	Magnitude range	b value	Reference (Fig.)
Predicted theoretically				
W model		< 5.0	2/3	
		5.0–5.7	1	
		5.7–6.6	2	
		> 6.6	3	
Single regression		> 4.5	1.70	Fig. 11(b)
		> 4.8	1.85	
		> 5	1.96	Fig. 11(a)
		> 5.3	2.02	
L model		< 5.0	2/3	
		5.0–5.7	1	
		5.7–6.6	2	
		> 6.6	3/2	
Single regression		> 4.5	1.47	Fig. 11(d)
		> 4.8	1.58	
		> 5	1.65	Fig. 11(c)
		> 5.3	1.76	
Observed (this study)				
CMT catalog 1977–1992 ($m_b > 4.5$)	8011	> 5.3	1.91	Fig. 12(a)
		5.3–5.7	1.17	Fig. 12(b)
		5.7–6.6	1.88	Fig. 12(b)
		> 6.6	2.83	Fig. 12(b)
First half	4005	> 5.3	1.80	
		5.3–5.7	1.15	
		5.7–6.6	1.90	
		> 6.6	2.11	
Second half	4006	> 5.3	1.88	
		5.3–5.7	1.20	
		5.7–6.6	1.86	
		> 6.6	4.89	
Odd only	4006	> 5.3	1.84	
		5.3–5.7	1.17	
		5.7–6.6	1.83	
		> 6.6	2.56	
Even only	4005	> 5.3	1.94	
		5.3–5.7	1.18	
		5.7–6.6	1.93	
		> 6.6	3.04	
NEIC catalog 1968–1991 ($m_b \geq 3$)	90074	> 4.8	1.82	Fig. 12(c)
		5.0–5.7	1.35	Fig. 12(d)
		5.7–6.6	2.04	Fig. 12(d)
		> 6.6	2.14	Fig. 12(d)
First half	45037	4.8–8.2	1.72	
		5.0–5.7	1.33	
		5.7–6.6	1.96	
		> 6.6	1.84	
Second half	45037	4.8–8.2	1.76	
		5.0–5.7	1.37	
		5.7–6.6	2.00	
		> 6.6	4.12	

Table 4 (continued)

Dataset or model	No. of samples	Magnitude range	b value	Reference (Fig.)
Odd only	45037	4.8–8.2	1.83	
		5.0–5.7	1.36	
		5.7–6.6	1.92	
		> 6.6	3.03	
Even only	45037	4.8–8.2	1.73	
		5.0–5.7	1.34	
		5.7–6.6	2.03	
		> 6.6	1.49	

$m_b \geq 3$. Fig. 12(c) indicates that the dataset is probably complete for $m_b \geq 4.8$. A single regression of the dataset above that threshold yields $b = 1.82$, in excellent agreement with the W model (1.85). When regressed in steps, the results generally uphold those of the CMT dataset: robust values of 1.35 and 2.04 for the predicted $b = 1$ and $b = 2$ ranges, and, in the predicted $b = 3$ range, an unstable figure varying between 1.8 and

4. It is interesting to note that for both the NEIC and CMT datasets, the largest b values in that range (4.12 and 4.89) are obtained when isolating the most recent events; the smallest (1.84 and 2.11) when considering the earliest events in the dataset. This could reflect a more accurate determination of magnitudes (notably a more stringent use of periods of the order of 1 s). In neither the CMT dataset nor the NEIC one was it possible to
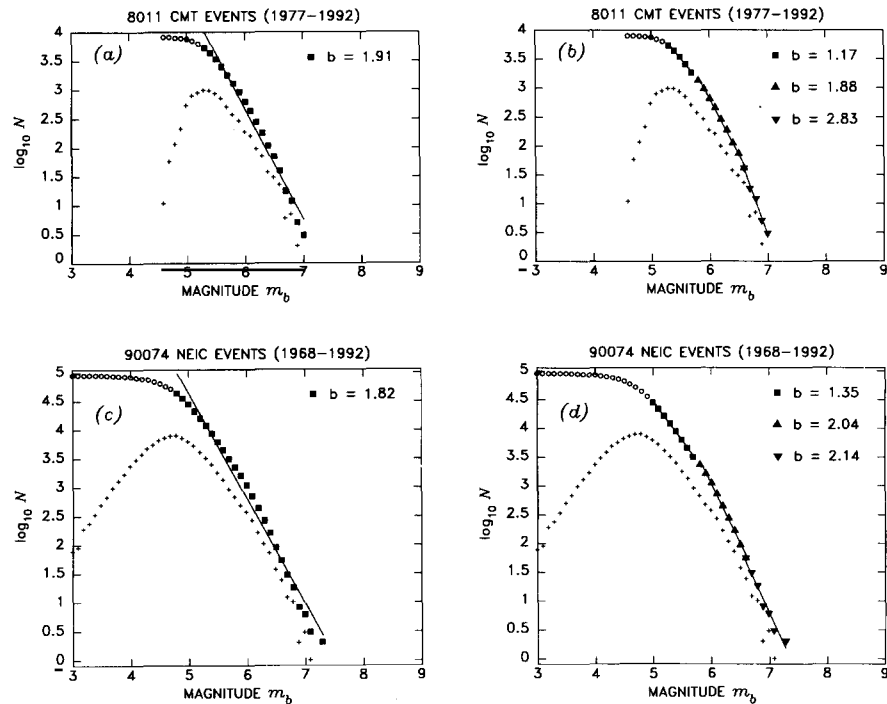

Fig. 12. Same as Fig. 9 for the body-wave magnitude m_b. Comparing (a) with Figs. 11(a) and 11(c), and (c) with Figs. 11(b) and 11(d), clearly favors the W model.
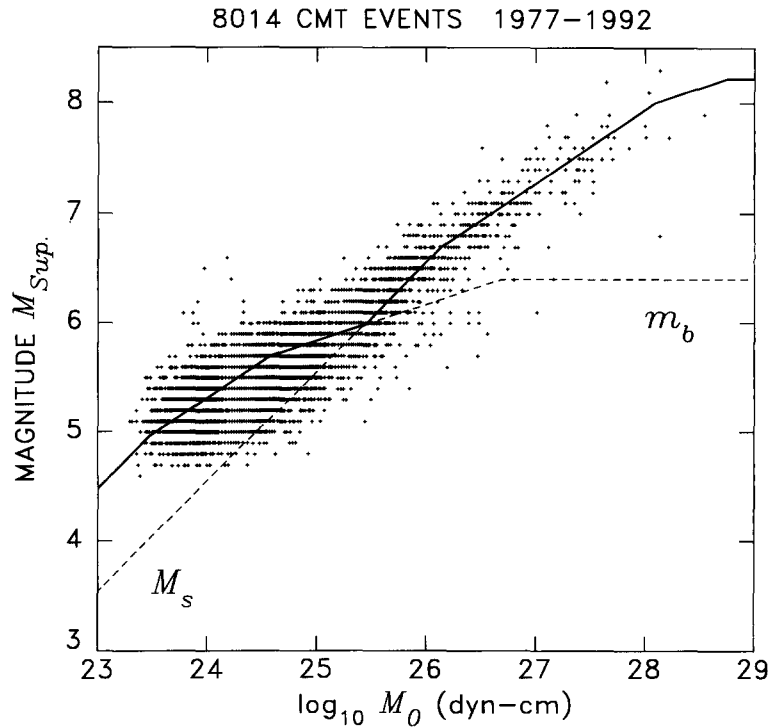
Fig. 13. Same as Fig. 10, except that the magnitude plotted is M_{Sup}, for each event the larger of M_s and m_b. Superimposed are the theoretical curves predicted for both M_s and m_b by Eqs. (9) and (11). The solid line is the predicted curve for M_{Sup}.

resolve the predicted $b = 2/3$ for smaller values of m_b, owing to incompleteness of the catalogs in that range of magnitudes.

4. Discussion

At this point, we have shown that a b value of unity is both predicted theoretically and observed experimentally (on homogeneous magnitude datasets) only under exceptional circumstances, namely over narrow ranges where a particular magnitude scale is undergoing partial saturation, leading to $\alpha = 2/3$. In the case of M_s, significant curvature is present in the frequency–magnitude relationship, and the b value varies from about two-thirds around $M_s = 5$ to a maximum of two just before total saturation, in the vicinity of $M_s = 8$. In the case of m_b, the range $b = 2/3$ cannot be studied on world-wide datasets as cata-

logs are incomplete at those lower magnitudes. A b value in the neighborhood of two is both predicted and observed at the $m_b = 5$–7 level.

The question then arises as to why empirical regressions of frequency–magnitude relationships can and do indeed yield $b = 1$, often with an acceptable fit. We believe this is due to the practice, commonly used by reporting agencies, of using a non-uniform magnitude scale, e.g. M_s for larger earthquakes and m_b for smaller ones, and indeed, often a local magnitude M_L for even smaller events, along the lines of Hanks and Kanamori (1979). Their procedure was designed to remain forcibly (and somewhat artificially) inside the domain $\alpha = 2/3$ over a broader range of magnitudes than would be predicted from the use of a single, uniform scale. In practice, this often amounts to retaining the largest available magnitude.

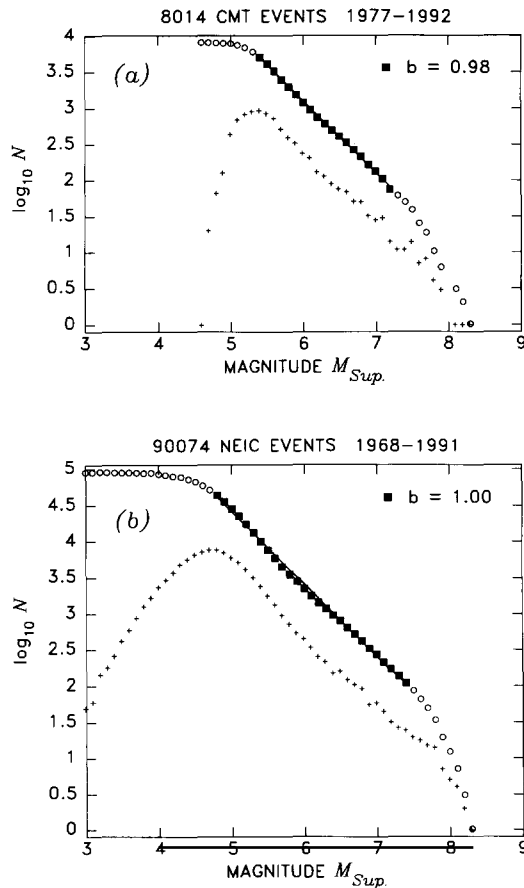To test this suggestion, we consider once again

Fig. 14. *b* values obtained from the CMT (a) and NEIC (b) datasets by using M_{Sup} (note that a *b* value close to 1.0 is achieved in both instances for moderately large events).

the CMT database and plot in Fig. 13 the larger $(M_{Sup.})$ of m_b and M_s, vs. $\log_{10} M_0$ for the 8014 shallow earthquakes with $M_{Sup} \geq 3$. The slope of the best-fitting regression, $M_{Sup} = 0.59 \log_{10} M_0 - 8.99$, is close to two-thirds, and thus we anticipate a *b* value close to unity. Indeed, Fig. 14(a) shows that the result of a single straight-line regression of this dataset is $b = 0.98$ for $M_{Sup} < 7.2$. The artifact of using a non-uniform magnitude scale eliminates both the range $b = 2$ (m_b) and the range $b = 2/3$ (M_s). These results are basically unchanged when considering the entire NEIC dataset of 90 074 earthquakes used in the

m_b study: as shown in Fig. 14(b), a perfect $b = 1.00$ is actually achieved in this case.

4.1. Comments on catalog completeness

Finally, we wish to comment on a rather surprising and intriguing aspect of the databases used in the present study. A comparison of their populations shows, for example, that among the 8015 shallow CMT solutions, only 6432 had a value of M_s quoted in the CMT file. In other words, 1583 (or roughly 20% of the whole population) did not. One would expect these to be generally small, a situation which could conceivably introduce a bias when comparing the results of β value studies on the whole dataset, and *b* values on the restricted one. However, the surprising result is that these 'no-M_s' CMT events are spread across all ranges of moment, their own β value being 0.84 between 10^{24} and 3×10^{28} dyn cm, generally comparable with those computed in Section 2. This property is further confirmed by the fact that β value studies of the two datasets yield virtually identical results, and further suggests that the absence of M_s from the CMT files is largely unrelated to earthquake size, and could result simply from random omissions. Indeed, we were able to assign 380 M_s values by simply matching the events with their NEIC catalog entries; further spot checks indicated that many events had International Seismological Centre (ISC) or other reported M_s. Although the apparently random character of the omissions shields our studies from systematic biases, it sheds some disturbing light on the whole question of catalog completeness.

In the case of m_b, the situation is at first sight much better, as all but four of the CMT solutions report an m_b. To a large extent, this was to be expected, as an m_b threshold is used to select earthquakes for CMT inversion. Of the four, three list an M_s value, and indeed all four have both m_b and M_s listed in the NEIC files, making it obvious that the omission is the result of a clerical error. At any rate, the number of events, as well as their small size ($M_0 \leq 3.4 \times 10^{24}$ dyn cm), effectively guards against affecting our analyses.

5. Conclusions

(1) A simple theoretical model of the effects of source finiteness predicts that for any conventional magnitude scale measured at a fixed period, the frequency–magnitude relationship should exhibit curvature resulting in an increase in b from two-thirds at lower magnitudes to higher values for larger magnitudes. A b value of unity is expected only in a restricted range of magnitudes; in this respect, it should be the exception, not the rule. For this reason, the interpretation of b values in terms of geological processes responsible for seismicity must take into account both the nature and the range of the magnitudes involved.

(2) Independently of this effect, fault width saturation results in a change of β value further affecting the b value of any magnitude scale. As pointed out by Romanowicz and Rundle (1993), simultaneous saturation of the fault slip Δu according to the W model predicts an increase in b value, whereas the L model in which fault slip keeps increasing predicts a decrease.

(3) The analysis of large catalogs of homogeneous magnitude datasets upholds the theoretical predictions. In particular, the CMT catalog clearly favors the W model over the L model, the latter predicting a decrease in β value at higher moments. Populations of surface-wave magnitudes M_s feature a b value of two-thirds at low magnitude ranges, increasing to about $b = 2$ before the onset of fault width saturation. Populations of body-wave magnitudes m_b are generally characterized by high b values, ranging from 1.35 to more than two; the expected domains of lower b values (one and two-thirds) are not observed on world-wide datasets because they would occur at ranges of m_b where catalogs are notoriously incomplete.

(4) When sorted by focal mechanism, normal faulting earthquakes fail to exhibit the sharp increase in β value observed for thrust faults, leading to the speculation that the former may escape fault width saturation; the present population of CMT mechanisms is, however, too small to allow definite conclusions in this respect. Strike-slip mechanisms exhibit a relatively continuous and smooth increase of their β value, suggesting a non-uniform saturation width. When further sorted according to tectonic environment, events along major continental strike-slip faults show a transition from $\beta = 2/3$ to higher values at a moment range smaller than the global dataset.

(5) The fact that a b value of unity is widely obtained and reported stems from the use of inhomogeneous magnitude catalogs, in which low and high values are measured using different scales (e.g. M_s for large events and m_b for smaller ones).

Acknowledgments

Appendix

We seek to justify the use of Eqs. (8) in the presence of physical saturation of the width W of the source, and in the W model, of the slip Δu. We proceed by briefly recalling the modeling of the saturation of M_s in the formalism of Geller (1976). The spectral amplitude of a surface wave at angular frequency ω is given by

$$X(\omega) = AM_0 \cdot \mathrm{sinc}\frac{\omega\tau}{2} \cdot \mathrm{sinc}\frac{\omega L}{2v_R}\mathrm{sinc}\frac{\omega W}{\pi C}$$

$$= A\mu\left(\Delta u \cdot \mathrm{sinc}\frac{\omega\tau}{2}\right) \cdot \left(L\,\mathrm{sinc}\frac{\omega L}{2v_R}\right)$$

$$\cdot \left(W\mathrm{sinc}\frac{\omega W}{\pi C}\right) \tag{A1}$$

where v_R is the velocity of rupture, A is a slowly varying function of ω, and $\mathrm{sinc}(x) = \sin x/x$. M_s is assumed to be proportional to $\log_{10} X(\omega_{20})$, where $\omega_{20} = 2\pi/20$ rad s^{-1}. Its saturation is explained by modeling $\log_{10} \mathrm{sinc}(x)$ as zero for x less than a corner value x_c and $\log_{10}(x_c/x)$ for $x \geq x_c$. In practice, $x_c = 1$.

In the absence of physical saturation of the

source, and as the size of the earthquake keeps increasing, each of the three terms in parentheses in (A1) will start by growing proportionally to L, but will saturate at a constant value when the argument of the sinc function becomes unity, i.e. when a certain corner angular frequency, ω_c, characteristic of each term, becomes less than ω_{20}. In the context of scaling laws, this is easily seen for the second and third terms. For the first one, $\omega_c = 2/\tau$, where τ is the rise time of the source. That the term saturates requires that the dislocation velocity $\Delta \dot{u} = \Delta u / \tau$ be constant, in other words that τ itself scale linearly with source dimension L. Under this assumption, which has often been described in the literature (Burridge, 1969; Brune, 1970; Kanamori, 1972; and more recently for very small events, Iio et al., 1993), the magnitude M_s saturates when the largest of the three characteristic corner frequencies becomes smaller than ω_{20}.

If we now assume a model with physical saturation of source parameters (either W in the case of the L model, or both W and Δu in the case of the W model), the effect of the saturation is simply to force the constancy of the relevant term(s) in parentheses in (A1). Once again, this is evident for the third term, and follows for the first one in the case of the W model from the assumption of constant dislocation velocity. It should be noted that the critical moment at which physical saturation of source width takes place ($M_0^c = 2 \times 10^{27}$ dyn cm) is greater by about a factor of ten than that separating the regimes (8a) and (8b). Thus, in the case of the W model, we predict immediate saturation of M_s at the critical moment M_0^c, whereas in the case of the L model, the slope in (8) should change to one-third until the first term in parentheses eventually saturates.

In this respect, it is difficult to reconcile the saturation of M_s around 8.2 and $M_0 \geq 10^{28}$ with the evidence obtained in Section 2 in support of the W model, as the latter would predict full saturation of M_s around 7.5 and for $M_0 \geq M_0^c$. We believe that this inconsistency must express the violation of one or more of the scaling assumptions used in the derivation of (A1), in the case of truly large earthquakes. In particular, the sinc functions in (A1) assume a homogeneous density of seismic moment release, both in the time domain (through the use of a ramp function), and in the spatial domain; this is contrary to a growing body of evidence which indicates a population of discrete asperities releasing most of the seismic moment (e.g. Houston, 1987; and more recently Wald and Heaton, 1993). In general, these effects will allow M_s to keep growing beyond its level of theoretical saturation.

In addition, some of the very largest earthquakes involved in Geller's (1976) study are normal faulting events (Sanriku, 1933; possibly Tokachi-Oki, 1952); we suggest in Section 2 that this population may not undergo width saturation for the same value of M_0^c, if at all. Also, several of the very large shocks in Geller's study are historical events whose moment determination may be inaccurate (e.g. Kanto, 1923; Sanriku, 1933; Nankaido, 1946), as suggested by independent measurements of mantle magnitudes at very long periods (Okal, 1992).

In conclusion, although Eq. (8) are difficult to justify in the framework of the physical saturation of W, they probably result from the breakdown of simplifying assumptions for a group of a few very large, mostly older, events. At any rate, Fig. 7 suggests that they provide a very good fit to the M_0–M_s relationship, for the available population of M_s values.

References

Brune, J.N., 1970. Tectonic stress and the spectra of seismic shear waves from earthquakes. J. Geophys. Res., 75: 4997–5009.

Burridge, R., 1969. The numerical solution of certain integral equations with non-integrable kernels arising in the theory of crack propagation and elastic wave diffraction, Philos. Trans. R. Soc. London, Ser. A, 265: 353–381.

Chinnery, M.A. and North, R.G., 1975. The frequency of very large earthquakes. Science, 190: 1197–1198.

Ekström, G. and Dziewonski, A.M., 1986. Evidence of bias in estimation of earthquake size. Nature, 332: 319–323.

Fitch, T.J., North, R.G. and Shields, M.W., 1981. Focal depths and moment tensor representations of shallow earthquakes associated with the great Sumba earthquake. J. Geophys. Res., 86: 9357–9374.

Frohlich, C. and Apperson, K.D., 1992. Earthquake focal mechanisms, moment tensors, and the consistency of seismic activity near plate boundaries. Tectonics, 11: 279–296.

Frohlich, C. and Davis, S.D., 1993. Teleseismic b-values; or, much ado about 1.0. J. Geophys. Res., 98: 631–644.

Geller, R.J., 1976, Scaling relations for earthquake source parameters and magnitudes. Bull. Seismol. Soc. Am., 66: 1501–1523.

Given, J.W. and Kanamori, H. 1980. The depth extent of the 1977 Sumbawa, Indonesia earthquake. EOS, Trans. Am. Geophys. Union, 61: 1044. (abstract).

Gutenberg, B. and Richter, C.F., 1941. Seismicity of the Earth. Geol. Soc. Am. Spec. Pap., 34, 131 pp.

Gutenberg, B. and Richter, C.F., 1954. Seismicity of the Earth. Princeton University Press, Princeton, NJ, 310 pp.

Hanks, T.C. and Kanamori, H., 1979. A moment magnitude scale. J. Geophys. Res., 84: 2348–2350.

Houston, H., 1987. Source characteristics of large earthquakes at short periods. Ph.D. Thesis, California Institute of Technology, Pasadena, CA, 150 pp.

Hyvernaud, O., Reymond, D., Talandier, J. and Okal, E.A., 1993. Four years of automated measurement of seismic moments at Papeete using the mantle magnitude M_m: 1987–1991. Tectonophysics, 217: 175–193.

Iio, Y, Ito, H., Sato, H., Ohminato, T., Kuwahara, Y. and Ando, M., 1993. Slow initial phase of the P-wave velocity pulse observed by a borehole seismometer on an earthquake fault. EOS, Trans. Am. Geophys. Union, 74 (43): 405. (abstract).

Kanamori, H., 1972. Determination of effective tectonic stress associated with earthquake faulting: the Tottori earthquake of 1943. Phys. Earth Planet. Inter., 5: 426–434.

Kanamori, H., 1977. The energy release in great earthquakes. J. Geophys. Res., 82: 2981–2987.

Lundgren, P.R. and Okal, E.A., 1988. Slab decoupling in the Tonga arc: the June 22, 1977 earthquake. J. Geophys. Res., 93: 13355–13366.

Lundgren, P.R., Okal, E.A. and Wiens, D.A., 1989. Rupture characteristics of the 1982 Tonga and 1986 Kermadec earthquakes. J. Geophys. Res., 94: 15521–15539.

Molnar, P., 1979. Earthquake recurrence intervals and plate tectonics. Bull. Seismol. Soc. Am., 69: 115–133.

Okal, E.A., 1989. A theoretical discussion of time-domain magnitudes: the Prague formula for M_s and the mantle magnitude M_m. J. Geophys. Res., 94: 4194–4204.

Okal, E.A., 1992. Use of the mantle magnitude M_m for the reassessment of the seismic moment of historical earthquakes. I: Shallow events. Pure Appl. Geophys., 139: 17–57.

Okal, E.A., 1993, m_b: A theoretical attempt at modeling the depth–distance correction. EOS. Trans. Am. Geophys. Union, 74 (16): 204 (abstract).

Okal, E.A. and Talandier, J., 1989. M_m: A variable period mantle magnitude. J. Geophys. Res., 94: 4169–4193.

Pacheco, J.F., Scholz, C.H. and Sykes, L.R., 1992. Changes in frequency–size relationships from small to large earthquakes. Nature, 355: 71–73.

Romanowicz, B.A., 1992. Strike-slip earthquakes on quasi-vertical transcurrent faults: inferences for general scaling relations. Geophys. Res. Lett., 19: 481–484.

Romanowicz, B.A. and Rundle, J.B., 1993. Scaling relations for large earthquakes. Bull. Seismol. Soc. Am., 83: 1294–1297.

Rundle, J.B., 1989. Derivation of the complete Gutenberg–Richter magnitude–frequency relation using the principle of scale invariance. J. Geophys. Res., 94: 12337–12342.

Scholz, C.H., 1982. Scaling laws for large earthquakes: consequences for physical models. Bull. Seismol. Soc. Am., 72: 1–14.

Silver, P.G. and Jordan, T.H., 1983. Total moment spectra of fourteen large earthquakes. J. Geophys. Res., 88: 3273–3293.

Turcotte, D.L., 1992. Fractals and Chaos in Geology and Geophysics. Cambridge University Press, Cambridge, 221 pp.

Wald, D.J. and Heaton, T.H., 1993. Landers — the movie. EOS, Trans. Am. Geophys. Union, 74(43): 429 (abstract).